Journal of the Chinese Institute of Engineers

ISSN: 0253-3839 (Print) 2158-7299 (Online) Journal homepage: www.tandfonline.com/journals/tcie20

Investigation of the sealing performance of the gearbox sealing system of high-speed trains

Shuai Shao, Kailin Zhang, Yuan Yao & Yu Zhang

To cite this article: Shuai Shao, Kailin Zhang, Yuan Yao & Yu Zhang (2023) Investigation of the sealing performance of the gearbox sealing system of high-speed trains, Journal of the Chinese Institute of Engineers, 46:1, 63-73, DOI: 10.1080/02533839.2022.2141335

To link to this article: https://doi.org/10.1080/02533839.2022.2141335

Published online: 11 Nov 2022.

JOURNAL OF THE CHINESE INSTITUTE OF ENGINEERS
2023, VOL. 46, NO. 1, 63–73
https://doi.org/10.1080/02533839.2022.2141335

MECHANICAL ENGINEERING

Investigation of the sealing performance of the gearbox sealing system of high-speed trains

Shuai Shao[a,b], Kailin Zhang[a], Yuan Yao[a] and Yu Zhang[c]

[a]State Key Laboratory of Traction Power, Southwest Jiaotong University, Chengdu, Sichuan, China; [b]State Key Laboratory of Heavy Duty AC Drive Electric Locomotive Systems Integration, CRRC Zhuzhou Electric Locomotive Co, Limited, Zhuzhou, Hunan, China; [c]No. 38 Research Institute, China Electronics Technology Group Corporation, Hefei, Anhui, China

ABSTRACT
Based on the analysis methods of lubricant–air separation and oil scavenging, a discrete phase model (DPM) considering droplet–wall interactions is used to analyze lubricant–air separation effectiveness, the volume of fluid (VOF) is used to analyze oil-scavenging effectiveness, and the sealing mechanism of the gearbox sealing system of high-speed trains is comprehensively studied. This study shows that the sealing effectiveness is influenced by the lubricant–air separation effectiveness and the oil-scavenging effectiveness. The separation effectiveness depends on the air drag force and the inertia of the lubricant droplets. The oil-scavenging effectiveness is related to the distribution of the lubricant after separation. In addition, with increasing lubricant droplet size, the sealing effectiveness first decreases and then increases, and the sealing system has the highest sealing effectiveness for medium-diameter droplets. The lower the outlet pressure is, the lower the sealing efficiency of the sealing system.

ARTICLE HISTORY
Received 15 November 2021
Accepted 28 August 2022

CO EDITOR-IN-CHIEF
Chen, ping-Hei

ASSOCIATE EDITOR
Jeng, Yeau-Ren

KEYWORDS
Gearbox sealing system; discrete phase model (DPM); droplet–wall interaction model; volume of fluid (VOF); sealing effectiveness

1. Introduction

Gearbox sealing is a key technology in the design process of high-speed train gearbox. Its sealing performance directly affects the safety and reliability of high-speed train. The gearbox has the characteristics of high speed and large load, which necessitates its lubrication with diluted oil. In addition, the high-speed operation of the gearbox increases the temperature of the lubricant and the inlet pressure of the sealing system, which facilitates the leaking of the lubricant from the gap between the end cover and the transmission shaft. To ensure the reliability of the gearbox, a non-contact labyrinth seal is often used.

As a classical sealing method, labyrinth seals are widely used in industrial gearboxes, rail transit gearboxes, wind power gearboxes and other transmission equipment. Many researchers have studied the sealing performance of labyrinth seals from the perspective of structural parameters, such as the number of labyrinth seal cavities, seal tooth profile angle and seal clearance (Feng et al. 2018; Kim and Cha 2009; Tang, Wang, and Zhao 2015). Wu and Andrés (2019) studied the influence of the sealing tooth position of the clearances on the sealing performance. The results showed that the interlocking straight labyrinth seal with teeth on both the rotor and stator had the least leakage. Kong et al. (2020) analyzed the effect of rotational speed and seal clearance on the inter-stage leakage characteristics of axial compressors. Compared with seal clearance, rotational speed has less of an effect on leakage. In the above research, an ideal gas is used as the sealing medium, but the sealing medium of the gearbox sealing system is a mixture of lubricant and air. An analysis of the sealing performance of a gearbox sealing system with the assumption of an ideal gas as the sealing medium is insufficient. It is necessary to analyze the sealing performance of the sealing system with a lubricant–air mixed medium. Li, Fang, and Li (2019) analyzed the sealing performance of three kinds of non-contact labyrinth seals when the compressor was running in a wet environment. The results showed that with an increase in liquid volume fraction in the mixed medium, the total leakage increased nearly linearly, but the gas leakage decreased. The results also showed that it was unreasonable to use an ideal gas instead of a mixed medium to study the sealing performance of gearbox sealing systems. He, Wang, and Zhang (2015) analyzed the flow field of a gearbox sealing system with an oil-gas two-phase mixed medium and studied the influence of the sealing clearance on leakage. However, in his study, only a two-dimensional flow field model was established, without considering the scavenge structure.

The above studies on labyrinth seal mechanisms are analyzed from the perspectives of energy conversion and kinetic energy dissipation. The non-contact three-cavity labyrinth dynamic seal used in the HTS gearbox includes a labyrinth seal and a scavenge structure. The two-phase lubricant–air mixture enters the labyrinth seal and passes through a series of throttling clearances and expansion cavities. The energy of the lubricant–air mixture is transformed and dissipated, and the separation of the lubricant is realized. The lubricant droplet separates from the lubricant–air mixture drops on the wall surface of the sealing cavity to form a lubricant film and flows back to the gearbox through the scavenge port. Therefore, it is

CONTACT Shuai Shao swjtushaoshuai@163.com State Key Laboratory of Traction Power, Southwest Jiaotong University, Chengdu, China

necessary to analyze both the separation effectiveness of labyrinth seals for lubricant droplets in lubricant–air mixtures and the oil-scavenging effectiveness after separation from the viewpoint of 'lubricant–air separation and oil scavenging' and to comprehensively evaluate the sealing effectiveness of gearbox sealing systems.

Many studies on the separation effectiveness of oil-gas separators have been conducted by using the oil-gas separation method. Wen et al. (2012) and Wen et al. (2016) applied a discrete phase method to analyze the separation effectiveness of supersonic cyclone separators. In their analysis, particles were divided into three groups depending on their trajectories: particles directly colliding with the wall, particles directly entering the collection area and particles directly passing through the diffuser. They also improved the separation effectiveness of the separator by setting a delta wing. Zhu and coworkers applied this method to study the separation effectiveness of a quick-contact cyclone reactor for particles with different diameters (Zhu, Li, and Wang 2017). The results showed that this method could provide a corresponding research basis for studying the mixing and separation mechanisms of cyclone separators. Misiulia and coworkers used an artificial neural network method to optimize the geometric parameters of a deswirler for cyclone separators (Misiulia, Elsayed, and Andersson 2017). Farrall et al. (2004) and Farrall et al. (2006) regarded the medium in the bearing chamber of an aero-engine as a mixture of oil and gas, considered the interaction between the airflow and the lubrication oil, and predicted its exit flow rate. The predicted results were very close to the experimental results, which further illustrated the feasibility of this research method. Based on a discrete phase model, Zhang and coworkers considered the interaction between the oil droplets and the walls and analyzed the sealing performance of the transmission sealing system of a gearbox with regard to the operating condition parameters and structural parameters of a labyrinth seal (Zhang, Zhang, and Yao 2019a, 2019b). However, in this study, only the separation effectiveness of the sealing system for the lubricant–air mixture was regarded as the sealing effectiveness, and the secondary leakage caused by the separated lubricant was not considered. For the sealing system of an HTS gearbox, the separation of lubricant from the lubricant–air mixture is the premise of sealing, and the effective return of the separated lubricant is paramount.

In this paper, a discrete phase model based on the Euler–Lagrange method and involving the consideration of droplet–wall interactions is used to analyze the separation effectiveness of a gearbox sealing system for lubricants in lubricant–air mixtures. Furthermore, the oil-scavenging effectiveness of the gearbox sealing system with respect to the separated lubricant deposited on the sealing cavity wall is analyzed. The sealing performance of the gearbox sealing system is evaluated by combining the separation effectiveness and the oil-scavenging effectiveness. Finally, the influence of the lubricant droplet size and the outlet pressure on sealing performance is studied.

2. Numerical model

The lubricant–air mixture flows in a sealing system under the pressure difference between the inside and the outside of the gearbox. Due to the throttling and friction effects of the labyrinth seal, the kinetic energy of the mixed medium is dissipated in the form of a strong eddy, and the lubricant droplets impinge on the wall to realize lubricant–air separation. The separated lubricant will form a lubricant film on the wall of the sealing cavity, and under the action of gravity and the interfacial shear force of air flow, it will flow back into the gearbox through the scavenge port.

2.1. Turbulence model

After passing through the inlet clearance, the sealing medium enters the sealing cavity at a high speed and forms a main vortex and multiple small vortices opposite to the direction of the main vortex. The renormalization group (RNG) *k-ε* turbulence model takes into account the influence of the eddy current on the turbulence and improves the equation of the turbulent kinetic energy dissipation rate so that it can effectively solve for the unstable vortex between the seal teeth. Therefore, the RNG *k-ε* turbulence model is more suitable for the numerical analysis of the flow field of the gearbox sealing system. The RNG *k-ε* turbulence model government equations are expressed as:

$$\frac{\partial(\rho k)}{\partial t} + \frac{\partial(\rho k u_i)}{\partial x_i} = \frac{\partial}{\partial x_j}\left[\alpha_k \mu_{eff} \frac{\partial k}{\partial x_j}\right] + G_k + \rho\varepsilon, \quad (1)$$

$$\frac{\partial(\rho\varepsilon)}{\partial t} + \frac{\partial(\rho\varepsilon u_i)}{\partial x_i} = \frac{\partial}{\partial x_j}\left[\alpha_\varepsilon \mu_{eff} \frac{\partial \varepsilon}{\partial x_j}\right] + \frac{C^*_{1\varepsilon}\varepsilon}{k} G_k - C_{2\varepsilon}\rho\frac{\varepsilon^2}{k}. \quad (2)$$

where ρ is the density, k is the turbulent kinetic energy, u is the velocity component in the x direction, and ε is the dissipation rate of turbulent kinetic energy. μ_t is the turbulence viscosity, μ is the fluid viscosity, μ_{eff} is the RNG *k-ε* turbulence model for turbulence viscosity correction, and $\mu_{eff} = \mu + \mu_t$.G_k is the generation term of the turbulent kinetic energy caused by the average velocity gradient. $C^*\ 1\varepsilon$ is the correction coefficient of the RNG *k-ε* turbulence model constant $C_{1\varepsilon}$.α_k and α_ε are the model constants of the turbulence model. t and x represent time and the x-axis displacement, respectively. The lower scales i and j are used to distinguish the difference before and after the correction of turbulent viscosity.

2.2. Two-phase flow model

Due to the churning effect of the gears and bearings, the lubricant is mixed with the air in the gearbox to form a gas–liquid two-phase flow. This flow state has a great impact on the working performance of the bearing sealing cavity and the gearbox. Therefore, a two-phase flow should be used when analyzing the sealing effectiveness of gearbox sealing systems. The discrete phase model (DPM) is used to analyze the lubricant–air separation process, and the volume of fluid (VOF) is used to analyze the oil-scavenging process.

In the analysis of the separation process, the air is set as a continuous phase, the lubricant droplet is set as a discrete phase, and the two-way coupling between lubricant droplets and air is considered to track the trajectories of the lubricant droplets. By analyzing the forces acting on the lubricant droplets, the differential equations of lubricant droplet motion are listed in the Cartesian coordinate system, and the trajectory of a lubricant droplet is solved by the integral method. In the Cartesian coordinate system, the equilibrium equations of the discrete phase are as follows:

$$\frac{du_p}{dt} = F_D(u_c - u_p) + \frac{g(\rho_p - \rho)}{\rho_p} + F_{saf}, \tag{3}$$

$$F_D = \frac{18\mu_c}{\rho_p d_p^2}\frac{C_D R_{ep}}{24}, \tag{4}$$

$$R_{ep} = \frac{\rho_c d_p |u_p - u_c|}{\mu_c}, \tag{5}$$

$$C_D = a_1 + \frac{a_2}{Re_p} + \frac{a_3}{Re_p}. \tag{6}$$

where u_c and ρ_c are the continuous phase velocity and density, respectively; u_P and ρ_P are the discrete phase velocity and density, respectively; $_c\mu$ is the continuous phase viscosity; d_P is the discrete phase diameter; F_D is the drag force per unit particle mass; F_{saf} is the Saffman lift force; C_D is the drag coefficient; a_1,a_2 and a_3 are constants; and R_{ep} is the discrete phase Reynolds number.

The lubricant–air mixture is separated by the sealing structure, and after this separation, most of the lubricant will condense to form a lubricant film on the wall of the sealing cavities and flow back to the gearbox effectively through the scavenge port under the pressure gradient between the labyrinth seal and the gearbox. The VOF is used to analyze the oil-scavenging process. After lubricant–air separation is realized, it can be considered that the lubricant and air no longer permeate each other, which meets the use conditions of the VOF. In the process of solving, each phase needs to be treated separately, and a joint analysis should be established by ensuring that the sum of the volume fraction of each phase in each control volume is 1.

$$\frac{\partial \alpha_p}{\partial t} + u_i \frac{\partial \alpha_p}{\partial x_i} = 0. \tag{7}$$

where α_P is the volume fraction of the p-phase fluid and u_i is the velocity component.

2.3. Lubricant droplet–wall interaction model

The sealing ring in the gearbox sealing system rotates at a high speed and forms a stable inner core eddy current. The lubricant droplets impinge on the wall of the sealing cavity under the centrifugal force and airflow drag force. The state of lubricant droplets after impingement determines the separation effectiveness of the sealing system. Bai and Gosman (1995) pointed out that when a droplet impinges on a wall, the energy of the droplet is lost, and the state of the droplet changes after impingement. As shown in Figure 1, according to the state of the droplet after impingement, the droplet–wall interaction can be divided into four types, namely, stick, rebound, spread and splash, which are determined by the motion parameters and physical properties of the droplet and the physical properties of the wall.

According to the state of the wall, lubricant droplet–wall interactions can be divided into two categories: impingement on a dry wall and impingement on a wet wall. For the impingement on a dry wall, the droplets will immediately deposit onto the wall to form a lubricant film, and then the dry wall will be converted into a wet wall. Therefore, the wall of the sealing system can be regarded as a wet wall when analyzing the gearbox sealing system. It is impossible to splash when an oil droplet impinges on a wall (Zhang, Zhang, and Yao 2019a). Therefore, the state of the oil droplets after impingement on the wall of the seal cavity may be stick, rebound or spread, and the state transformation processes are shown in Table 1. The stick and spread lubricant droplets can be considered to be captured by the wall and to have formed a lubricant film during the separation process. For rebound droplets, Grant and Tabakoff (1975) introduced the rebound coefficients e_n and e_t to describe the kinetic energy changes before and after impingement:

$$e_n = 0.993 - 0.176\theta - 1.56\theta^2 - 0.49\theta^3, \tag{8}$$

$$e_t = 0.988 - 1.66\theta + 2.11\theta^2 - 0.67\theta^3. \tag{9}$$

2.4. Simulation parameter settings

This numerical simulation is carried out in the commercial software ANSYS Fluent 17.0 and Simerics MP+ 5.0. The separation process of the sealing system for the lubricant–air mixture medium is carried out in Fluent 17.0. In this process, the interaction between lubricant droplets and the wall is simulated by the user defined function denoted as DEFINE_DPM_BC. A two-way coupling analysis is used to consider the interaction between the lubricant droplet and the air. Considering the complexity of fluid flow in the sealing system and the convergence in the calculation process, the Semi-Implicit Method for Pressure Linked Equations (SIMPLE) algorithm is used to solve the Navier–Stokes equation, and a first-order upwind scheme is used to discretize the turbulence model in this paper.

The numerical results of the separation process are used as the boundary conditions for the analysis of the oil-scavenging process of the sealing system, which is carried out in Simerics

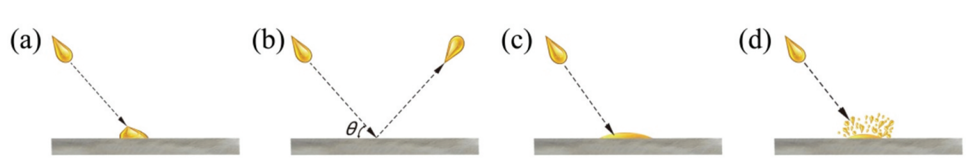

Figure 1. Lubricant droplet–wall interaction diagram. (a) stick; (b) rebound; (c) spread; (d) splash.

Table 1. State transformations of droplet after impingement on a wet wall.

State	Weber number
Stick→Rebound	$Wec \approx 1$
Rebound→Spread	$Wec \approx 5$
Spread→Splash	$Wec = 1320\,La^{-0.18}$

Table 2. Oil–gas separation effectiveness.

Blow-by flow (L/min)	100	122	179
Simulation	82.3%	84.4%	87.6%
Experiment	79.8%	83.3%	86.7%
Error	3.13%	1.32%	1.04%

MP+ 5.0. The default convergence residual standard of FLUENT and Simerics MP+ is adopted: it is considered that the calculation converges when the residual values of all variables are lower than 10^{-3}. In the process of numerical simulation, the workstation configuration we used has 64 GB memory and an Intel Xeon W-2155 CPU.

3. Experimental verification

To verify the applicability and accuracy of the proposed model, the modified model is applied to a gas engine labyrinth oil-gas separator for numerical calculation. The details of the labyrinth oil-gas separator, the experimental method and the boundary conditions are defined as previously described in the reference (Lu 2016). The inlet boundary condition adopts the velocity inlet, which is 0.504 m/s, 0.615 m/s and 0.902 m/s, and the corresponding blow-by flows are 100 L/min, 122 L/min and 179 L/min, respectively. The outlet boundary condition is adopted for the pressure outlet, and the outlet gauge pressure is −600 Pa. The numerical simulation results and experimental results of oil-gas separation efficiency of gas engine labyrinth oil-gas separator are shown in Table 2. Taking the blow-by flow as a variable, the up oil quantity m_{out} and return oil quantity m_{re} before and after the test are measured, and the sum of the two is taken as the blow-by flow m_{in}. The separation effectiveness is calculated by Equation (10):

$$\eta = \left(1 - \frac{m_{out}}{m_{in}}\right) \times 100\%. \tag{10}$$

4. Simulation model and conditions

4.1. Geometric model

The sealing system studied in this paper includes an axial seal, a radial seal and a scavenge structure, as shown in Figure 2. The axial seal is composed of the sealing clearance between a seal slinger and a shaft bushing, which is called cavity *I–III*. The radial seal is the clearance between a seal slinger and a shaft end over, which is mainly used to balance the pressure difference between the axial labyrinth seal and the environment so that more lubricant droplets can impinge on the wall surface of the seal cavity to realize separation.

The scavenge structure is a body size hole that penetrates the casing and the bushing. This structure mainly has two functions: on the one hand, it connects the axial seal with the inside of the gearbox, balances the pressure of the axial seal, causes the axial seal to form a stepped pressure distribution, and improves the effectiveness of lubricant–air separation; on the other hand, it is used to scavenge the lubricant after separation.

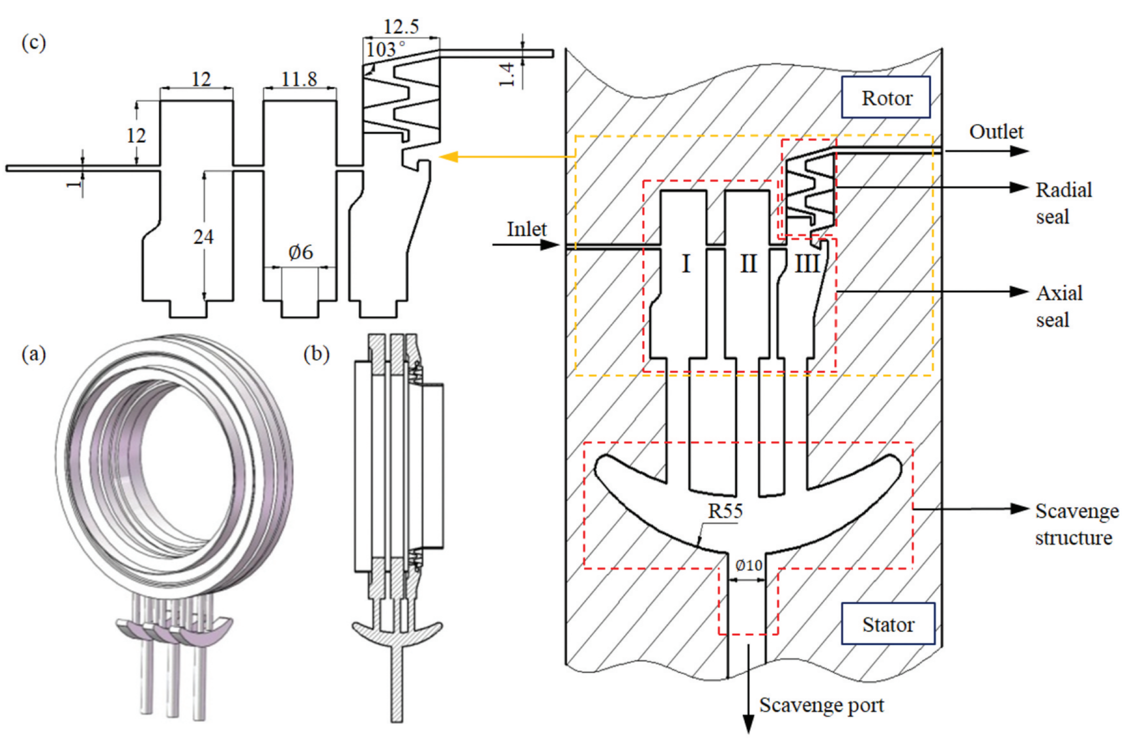

Figure 2. Sealing system diagram. (a) three-dimension diagram; (b) middle section diagram; (c) partial enlarged detail diagram.

4.2. Boundary conditions

The boundary conditions of the sealing system are determined by the flow field in the gearbox and the external environment. When the pressures of the inlet, outlet and scavenge port are stable, the leakage of the sealing system will be stable. The pressures of the inlet and scavenge port are based on the internal steady-state flow field under the rated conditions of the gearbox, and the outlet pressure adopts an empirical value of −600 Pa. According to the practical application of the gearbox, the lubricant used to analyze the internal flow field and the sealing system of the gearbox is 75 W-90, with a density of 866 kg/m^3 and a viscosity of 13.15 mm^2/s. The diameter of the lubricant droplet is set as 1–12 μm when studying the relationship between the droplet size and the sealing effectiveness.

When analyzing the separation effectiveness of the sealing system for lubricant–air mixtures, the DPM is adopted, in which the air is set as a continuous phase and the lubricant droplet is set as a discrete phase. When setting up the DPM, the escape boundary is used for the scavenge port and outlet; that is, when the lubricant droplets entrained by air are transported to the above boundary, it is considered that the droplets escape and are not relevant in subsequent calculations. For the other boundaries of the sealing system, the DEFINE_DPM_BC program is compiled to define the boundary condition of the lubricant droplets impinging on a rigid wall. The state of the droplets after impingement is calculated according to Equation (8) and Equation (9), and the subsequent motion is defined according to Table 1. When the flow field is stable, the lubricant particles adhering to the wall surface are counted as the lubricant distribution.

The lubricant leakage quantity of gearbox sealing system m_e consists of two parts: one is the lubricant that escapes from the outlet of the sealing system directly without separation m_{e1}, and the other is the lubricant that adheres to the wall surface of the sealing cavity after separation but without scavenging m_{e2}. The sealability of the sealing system is determined by the characteristics of the lubricant–air separation and oil-scavenging.

The calculation formula for the lubricant–air separation effectiveness of the gearbox sealing system is as follows:

$$\eta_{sep} = \left(1 - \frac{m_{e1}}{m_{in}}\right) \times 100\%. \tag{11}$$

The calculation formula for the oil-scavenging effectiveness of the gearbox sealing system is as follows:

$$\eta_{OR} = \left(1 - \frac{m_{e2}}{m_{in} - m_{e1}}\right) \times 100\%. \tag{12}$$

The calculation formula for the total leakage of the gearbox sealing system m_e is as follows:

$$m_e = m_{e1} + m_{e2}. \tag{13}$$

The sealing effectiveness of the gearbox sealing system is as follows:

$$\eta_{seal} = \left(1 - \frac{m_e}{m_{in}}\right) \times 100\%. \tag{14}$$

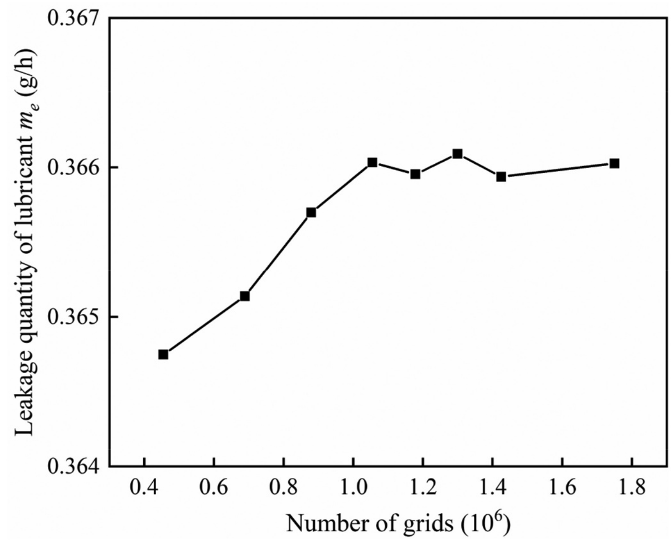

Figure 3. Grid Independence curve.

where m_{in} is the mass of all lubricant droplets entering the gearbox sealing system, m_{e1} is the lubricant leakage without separation, and m_{e2} is the leakage of lubricant after separation but without scavenging.

4.3. Grid Independence verification

To improve the calculation effectiveness as much as possible without affecting the calculation accuracy, it is necessary to use a suitable mesh size in the calculation model. The whole sealing system is meshed by an unstructured mesh, and a standard wall function is applied to the wall of the seal cavity. To ensure the preciseness of the numerical results, the mesh that has a great influence on the results, such as the sealing clearance, is locally refined. Taking m_e as a characteristic parameter, eight calculation grids with the number of grids from 0.35–1.69 million are selected, and the relationship between m_e and the number of grids is analyzed, as shown in Figure 3. With an increase in the number of grids, m_e increases gradually. When the number of grids increases to a certain amount, m_e tends to be stable, which shows that the number of grids has little influence on the simulation results. To ensure the calculation accuracy and the calculation effectiveness, the calculation model (the minimum grid size is 0.3 mm, and the maximum grid size is 3 mm) with 1.45 million grid units is selected for subsequent simulation analysis.

5. Results and discussion

5.1. Analysis of the sealing mechanism

The airflow in the sealing system interacts with the motion of lubricant droplets. According to the reference (Zhang, Zhang, and Yao 2019a), and by setting the same boundary conditions, the separation process of the sealing system for the lubricant–air mixture and the oil-scavenging process after separation are analyzed to study the sealing mechanism. The pressures at the inlet and scavenge ports of the sealing system are set to 580 Pa and 240 Pa, respectively, and the outlet pressure is set to an ambient back pressure of −600 Pa. The rotation speed of the seal ring is set to 1900 rpm. The lubricant–air mixture with a lubricant volume fraction of 7.72% is selected as the sealing medium. The diameter of the lubricant droplets is set to 6 μm. The internal flow field characteristics of the gearbox sealing system are numerically analyzed, and the pressure nephogram, velocity nephogram and lubricant droplet trajectory diagram of the lubricant–air separation process, as well as the pressure nephogram and velocity nephogram of the oil-scavenging process, are given in Figure 4.

Figure 4(a–c) show that the lubricant–air mixture enters the axial seal from the inlet at a high speed. Through the effects of throttling clearance and cavity dissipation, the pressure energy of the sealing medium is converted into kinetic energy, and then the kinetic energy is converted into thermal energy in the form of

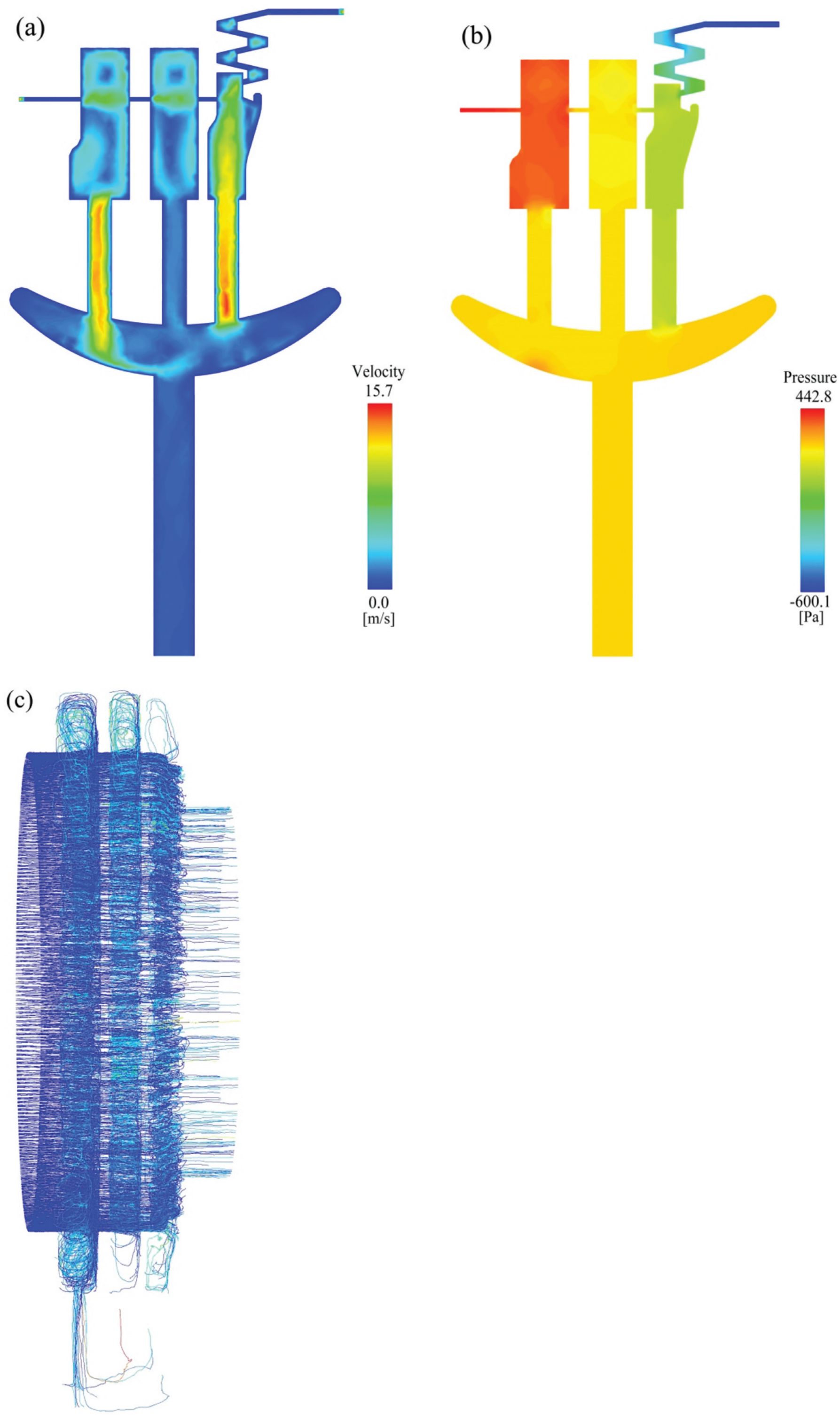

Figure 4. Characteristics of flow in the sealing system. (a) Pressure nephogram of separation; (b) Velocity nephogram of separation; (c) Lubricant droplet trajectory diagram; (d) Pressure nephogram of scavenging; (e) Velocity nephogram of scavenging.

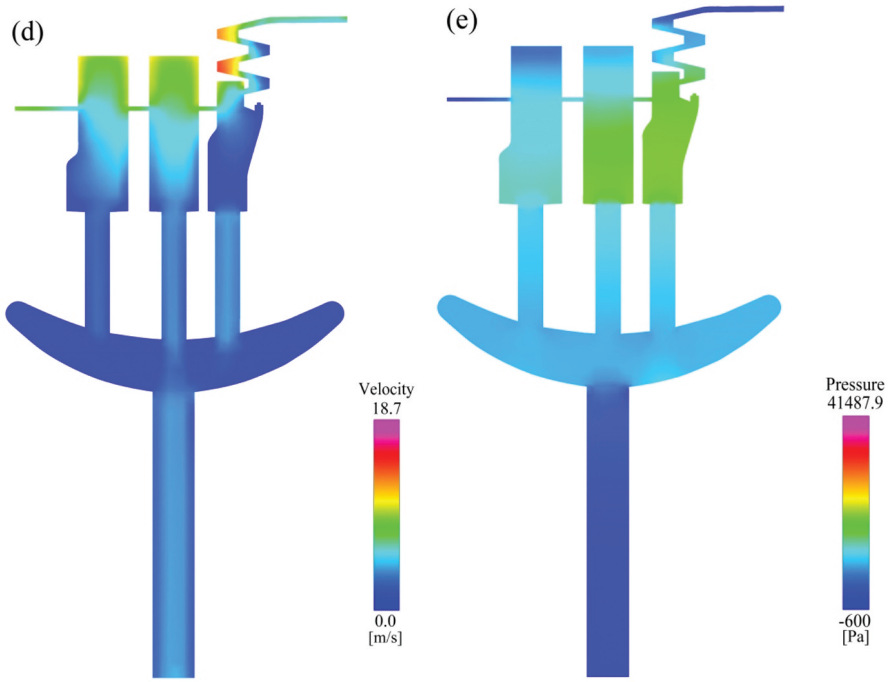

Figure 4. (Continued).

a cavity vortex for dissipation. In the processes of energy conversion and dissipation, due to the eddy currents in the sealing cavities, the trajectories of the lubricant droplets are changed, which results in the generation of an acceleration inertia force and causes the droplets to impinge on the wall surface. Therefore, the lubricant droplets are affected by the airflow drag force and their own inertia force. The inertia force of the droplets includes the inertial force related to acceleration and the inertial force related to mass. The stronger the drag effect of the airflow is, the more easily the lubricant droplets are wrapped and moved by the air, and the lower the lubricant–air separation effectiveness. The stronger the inertia force is, the stronger the abilities of the lubricant droplets to maintain their original motion, and the higher the lubricant–air separation effectiveness.

It can be seen from Figure 4(d,e) that after separation, lubricant droplets will form a lubricant film due to their immediate deposition on the wall of the sealing cavity, and after separation, the lubricant will flow back to the gearbox through the scavenge port to achieve effective backflow. However, some lubricant droplets that are close to the end of the axial seal cavity will accumulate into a large droplet or lubricant film and escape along the radial seal clearance under the pressure gradient between the labyrinth seal and the environment. Therefore, lubricant–air separation is a prerequisite for sealing, and the purpose of sealing is to achieve the effective return of lubricant after separation.

Table 3 shows the statistical data of the lubricant droplets trapped by the wall of each sealing cavity and the lubricant mass flows at the outlet and scavenge port after separation when the lubricant droplets with a diameter of 6 μm move in the sealing system according to the above boundary conditions. Table 3 shows that during the separation process, most lubricant droplets are trapped by the walls of the sealing system, and only a small number of lubricant droplets escape directly from the outlet without impingement on the wall surface of sealing cavity. The lubricant droplets trapped by the wall of the sealing system, most of which are separated by the wall of sealing cavity *I*, are considered as lubricant after effective separation. After separation, the oil-scavenging efficiency of the sealing system is analyzed according to the proportion of the separation efficiency of each sealing cavity to the lubricant–air mixture. And after separation, some lubricant will still escape from the outlet, resulting in secondary leakage. The lubricant flowing back to the gearbox from the scavenge port is considered to realize effective oil return.

5.2. Influence of lubricant droplet size

The trajectories of the lubricant droplets continuously change, which alters the lubricant–air separation effectiveness and scavenging effectiveness. The boundary conditions used in this section are consistent with *Section 5.1 Analysis of the sealing mechanism*. The separation effectiveness and oil-scavenging

Table 3. Quality statistics of lubricant.

	Inlet(g/h)	Cavity *I*wall (g/h)	Cavity *II*wall (g/h)	Cavity *III*wall (g/h)	Scavenge structure wall (g/h)	Outlet(g/h)
Separation progress	1.3824	0.4618	0.1453	0.0915	0.0006	0.0271
Scavenging progress	Inlet (g/h) 1.1948		Scavenge port (g/h) 0.703		Outlet (g/h) 0.4918	

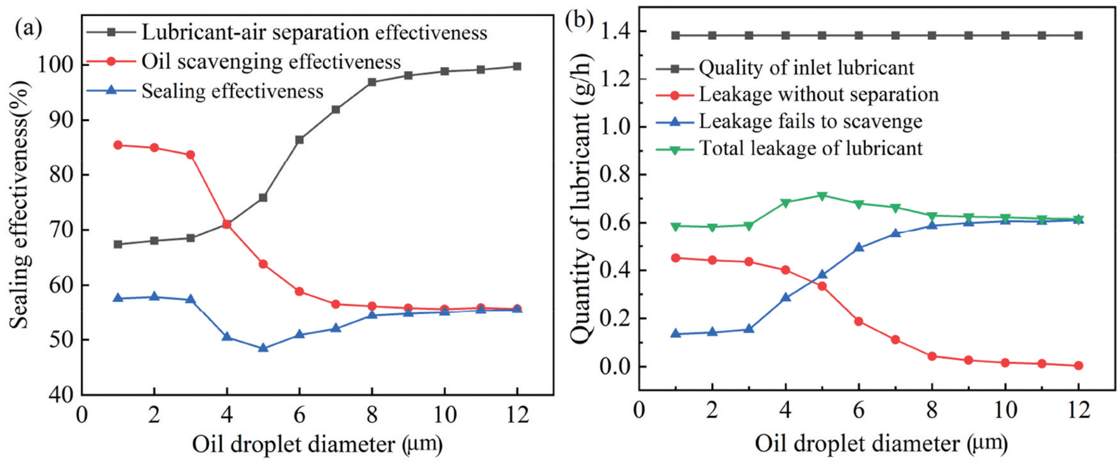

Figure 5. Relationship between sealing effectiveness and lubricant droplet size. (a) Sealing effectiveness; (b) Quantity of lubricant.

effectiveness are calculated to analyze the influence of the lubricant droplet size, with oil droplet diameters ranging from 1 to 12 μm, on the sealing effectiveness. The product of the separation effectiveness and scavenging effectiveness can be considered as the sealing effectiveness of the sealing system. Figure 5 shows the relationship between the sealing effectiveness and lubricant droplet size.

Figure 5 shows that with increasing oil droplet diameter, the separation effectiveness of the sealing system gradually increases, and the oil-scavenging effectiveness gradually decreases. Affected by the separation effectiveness and oil-scavenging effectiveness, the sealing effectiveness first decreases and then increases. The results show that the sealing effect of the sealing system is good for small and large diameter droplets, but it is poor for medium diameter droplets. This is due to the low separation effectiveness of the sealing system for small-diameter droplets. Some small-diameter lubricant droplets are not separated and leak directly from the sealing clearance. The amount of lubricant directly leaked without separation accounts for approximately 75% of the total lubricant leakage. With regard to an increasing oil droplet diameter, when the oil droplet diameter exceeds 3 μm, the separation effectiveness is significantly improved; that is, more lubricant is separated from the lubricant–air mixture, but the oil-scavenging effectiveness of the system is decreased, which makes the separated lubricant fail to return to the gearbox and causes leakage. When the oil droplet diameter continues to increase to 10 μm, the separation effectiveness is close to 100%; that is, the lubricant is almost completely separated, but at this time, the oil-scavenging effectiveness is low, so it can be considered that almost all the leakage comprises the lubricant that has not achieved effective scavenging.

When the boundary conditions of the sealing system are given, the oil-scavenging effectiveness is determined by the distribution of lubricant after separation. Figure 6 shows the separation effectiveness of each sealing cavity under two typical working conditions corresponding to the above lubricant droplet size change process. When the oil droplet diameter changes from 2 μm to 10 μm, the separation effectiveness of sealing cavity *I* and cavity *II* changes slightly, and the separation effectiveness of sealing cavity *III* increases significantly. This is because the drag force of the air flow is dominant during the movement of the small-diameter droplets, which makes it easier for these droplets to pass through the clearance between the seal tooth without impinging on the wall. During the movement of large-diameter droplets, the inertial force is dominant, which makes it easier for these droplets to maintain their original states of motion. Under this sealing structure, the straight-through effect of the sealing system is significant, and the

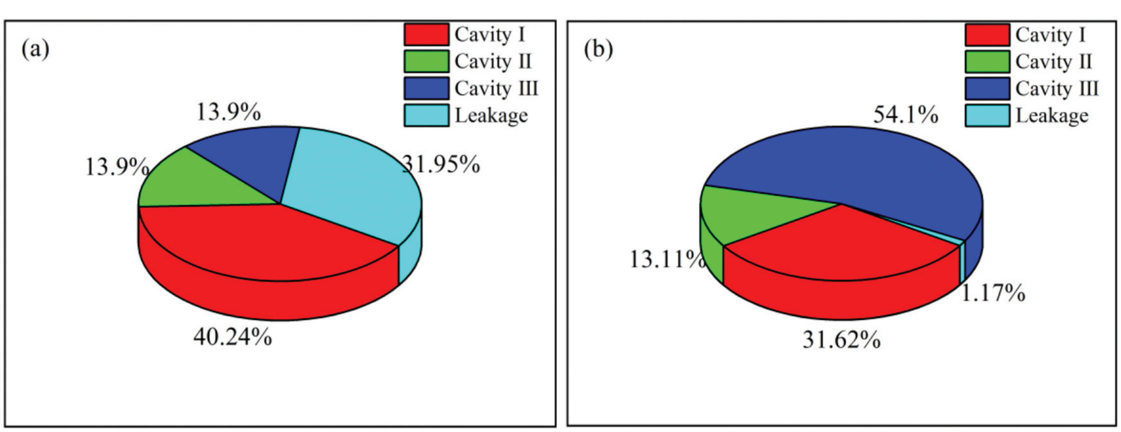

Figure 6. Separation effectiveness of each cavity with different oil droplet diameters. (a) 2 μm; (b) 10 μm.

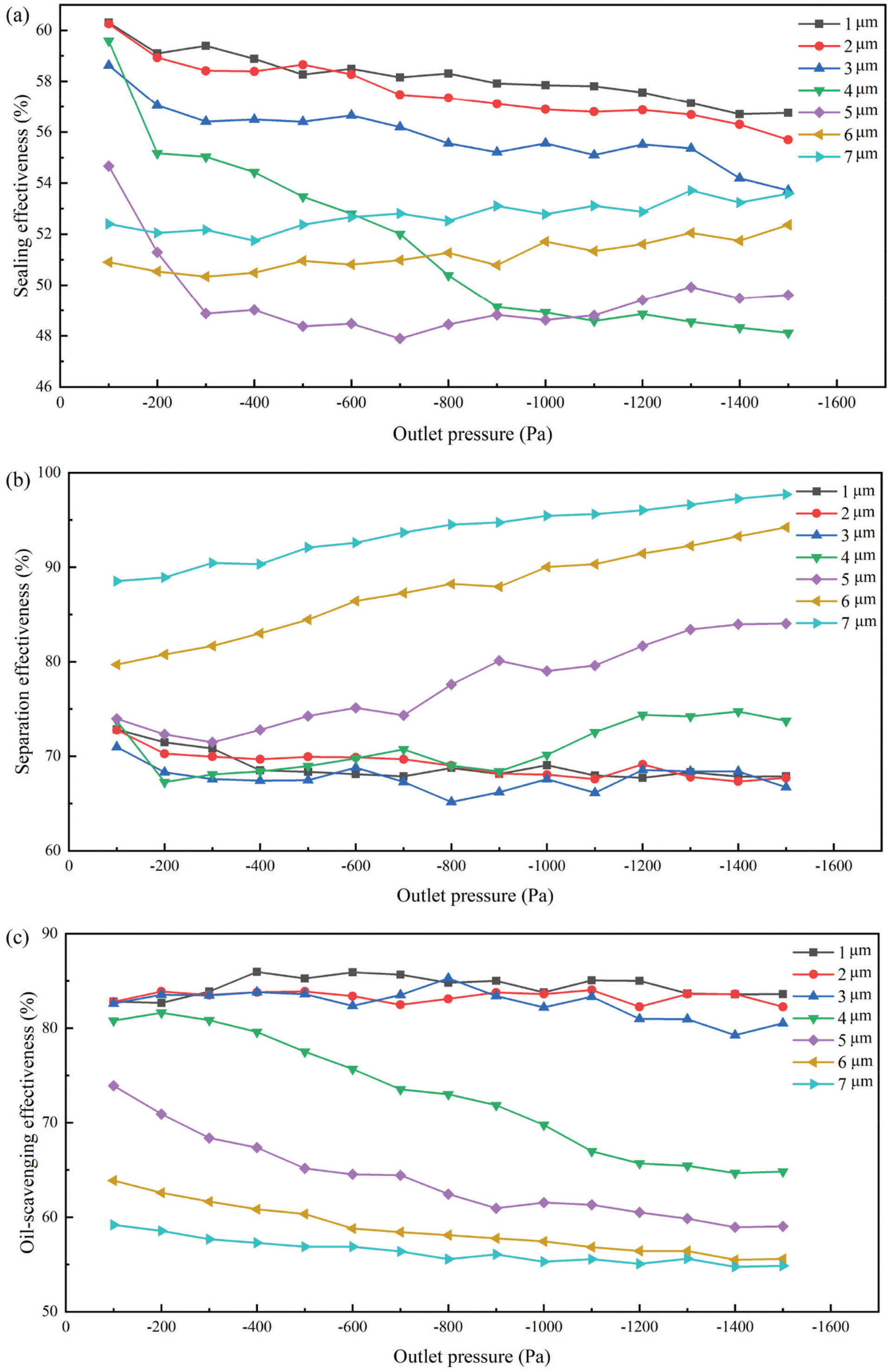

Figure 7. Relationship between sealability and outlet pressure. (a) Sealing effectiveness; (b) Separation effectiveness; (c) Oil-scavenging effectiveness.

lubricant droplets easily pass through cavity *I* and cavity *II* and into cavity *III*. The radial seal located at the tail-end of the seal system weakens the straight-through effect of sealing cavity *III*, allowing the vortex to form more easily, thereby enhancing both the possibility of lubricant droplet impingement on the wall and the separation of lubricant. The separated lubricant accumulates in sealing cavity *III*. If it cannot flow back to the gearbox in time, it will leak by way of the radial seal clearance.

5.3. *Influence of outlet pressure*

The pressures of the inlet, outlet and scavenge port of the sealing system are different. The pressures of the inlet and scavenge port are determined by the flow field in the gearbox, and the outlet pressure is related to the operating conditions and the external environment. The pressure difference between the inlet and the outlet is the key factor for generating fluid propulsion. Therefore, it is very important to study the relationship between this pressure difference and the sealing effectiveness. In this section, the pressure at the inlet and scavenge port are consistent with that in *Section 5.1 Analysis of the sealing mechanism*, and the outlet pressure is set to −100~-1500 Pa to study the sealability of the pressure different between the outlet and inlet of the sealing system on lubricant droplets with different diameters, as shown in Figure 7.

As the product of the separation effectiveness and oil-scavenging effectiveness, the sealing effectiveness should be analyzed from these two processes. The separation effectiveness is determined by the airflow drag force and inertia force. For small-diameter droplets, the drag force is dominant. Reducing the outlet pressure will accelerate the movement of these droplets in the sealing system. A greater number of lubricant droplets will not impinge on the wall and escape directly from the outlet. The separation effectiveness of each sealing cavity changes slightly. At this time, the sealing effectiveness of the system mainly depends on the lubricant–air separation effectiveness. The oil-scavenging effectiveness depends on the distribution of lubricant after separation. For large-diameter lubricant droplets, inertial force dominates, and these droplets will maintain their original states of motion. Reducing the outlet pressure will accelerate the movement of the lubricant droplets in the sealing cavity, allowing more lubricant droplets to impinge on the wall to realize separation and significantly improving the separation effectiveness of cavity *III* so that more lubricant accumulates at the inlet of the radial seal. Under the pressure difference between cavity *III* and the outlet, a portion of the separated lubricant escapes through the radial seal clearance. At this time, the sealing effectiveness depends on the oil-scavenging effectiveness.

6. Conclusion

This paper investigates the sealing mechanism of a gearbox sealing system from the perspective of 'lubricant–air separation and oil scavenging' and analyzes the effects of the lubricant droplet size and outlet pressure on the sealing effectiveness and the leakage of lubricant. Through the above analysis, the following conclusions are obtained:

The sealing effectiveness of the HST gearbox is determined by the separation effectiveness and oil-scavenging effectiveness. The lubricant leakage of the sealing system consists of two parts: the lubricant without separation, m_{e1}, and the lubricant after separation but without scavenging, m_{e2}.

The main factors affecting the separation effectiveness are the air drag force and its own inertial force. If the air flow drag force acting on the lubricant droplets is smaller or the inertia force is larger, the separation effectiveness of the sealing system is higher, which means that more lubricant will be separated from the lubricant–air mixture.

The scavenging effectiveness is mainly related to the distribution of lubricant after separation. The more lubricant that is separated from the sealing cavity *III*, the more lubricant that will leak from the radial seal clearance, and the lower the scavenging effectiveness of the system is.

As the lubricant droplet size increases, the sealing effectiveness decreases first and then increases. For small-diameter droplets, the separation effectiveness is low, and the leakage of lubricant is mainly m_{e1}. However, for large-diameter droplets, the separation effectiveness is improved, but the oil-scavenging effectiveness is low, and the leakage of lubricant is mainly m_{e2}.

With the decrease in outlet pressure, the sealing effectiveness decreases and the leakage increases, but its influence on lubricant–air separation effectiveness and oil-scavenging effectiveness is different.

Nomenclature

a_1, a_2, a_3	the constants of the drag coefficient C_D
$C_{1\varepsilon}$	the correction coefficient of the RNG k-ε turbulence model
$C^*{}_{1\varepsilon}$	the correction coefficient of the RNG k-ε turbulence model constant $C_{1\varepsilon}$
C_D	the drag coefficient
d_P	the discrete phase diameter
e_n	the normal rebound coefficients of rebound droplet
e_t	the tangential rebound coefficients of rebound droplet
F_D	the drag force per unit particle mass
F_{saf}	the Saffman lift force
G_k	the generation term of the turbulent kinetic energy caused by the average velocity gradient
k	the turbulent kinetic energy
m_e	the lubricant leakage quantity of gearbox sealing system
m_{e1}	the lubricant that escapes from the outlet of the sealing system directly without separation
m_{e2}	the lubricant that adheres to the wall surface of the sealing cavity after separation but without scavenging
m_{in}	the blow-by flow of the gas engine labyrinth oil-gas separator
m_{out}	the up oil quantity of the gas engine labyrinth oil-gas separator
m_{re}	the return oil quantity of the gas engine labyrinth oil-gas separator
R_{ep}	the discrete phase Reynolds number
t	the time
u	the velocity component in the x direction
u_c	the continuous phase velocity
u_i	the velocity component
u_P	the discrete phase velocity
x	the x-axis displacement
α_k	the model constants of the turbulence model
α_P	the volume fraction of the p-phase fluid
α_ε	the model constants of the turbulence model
ε	the dissipation rate of turbulent kinetic energy
η	the separation effectiveness of the gas engine labyrinth oil-gas separator
η_{OR}	the oil-scavenging effectiveness of the gearbox sealing system
η_{seal}	the sealing effectiveness of the gearbox sealing system
η_{sep}	the lubricant–air separation effectiveness of the gearbox sealing system
μ	the fluid viscosity
μ_c	the continuous phase viscosity
μ_{eff}	the RNG k-ε turbulence model for turbulence viscosity correction
ρ_P	the discrete phase density
μ_t	the turbulence viscosity
ρ	the density
ρ_c	the continuous phase density

Disclosure statement

No potential conflict of interest was reported by the author(s).

Funding

The material in this paper is based on work supported by National Railway Group Science and Technology Program grant (N2020J026, N2021J028), the Independent Research and Development Projects of State Key Laboratory of Heavy Duty AC Drive Electric Locomotive Systems Integration (R111720H01385), and the Independent Research and Development Projects of a Key Laboratory grant (2022TPL-T02).

ORCID

Shuai Shao http://orcid.org/0000-0001-5076-3477
Kailin Zhang http://orcid.org/0000-0003-1063-6793
Yuan Yao http://orcid.org/0000-0003-2279-7463
Yu Zhang http://orcid.org/0000-0003-0710-5828

Data availability statement

Some or all data, models, or code that support the findings of this study are available from the corresponding author upon reasonable request. (Testing data, codes for implemented models, and evaluation metrics). https://figshare.com/articles/dataset/Investigation_of_the_sealing_performance_of_the_gearbox_sealing_system_of_high-speed_trains/21435660

References

Bai, C., and A. D. Gosman. 1995. "Development of Methodology for Spray Impingement Simulation." *SAE Transactions* 104: 550–568. doi:10.4271/950283.

Farrall, M., S. Hibberd, K. Simmons, and D. Giddings. 2006. "Prediction of Air/Oil Exit Flows in a Commercial Aero-Engine Bearing Chamber." *Proceedings of the Institution of Mechanical Engineers. Part G, Journal of Aerospace Engineering* 220 (3): 197–202. doi:10.1243/09544100JAERO40.

Farrall, M., K. Simmons, S. Hibberd, and P. Gorse. 2004. "A Numerical Model for Oil Film Flow in an Aero-Engine Bearing Chamber and Comparison with Experimental Data." In *Proceedings of the ASME Turbo Expo 2004: Power for Land, Sea, and Air. Volume 4, Turbo Expo* Vienna, Austria, 14-17 June 2004, 409–417. New York: ASME.

Feng, J., L. Wang, H. Yang, and X. Peng. 2018. "Numerical Investigation on the Effects of Structural Parameters of Labyrinth Cavity on Sealing Performance." *Mathematical Problems in Engineering* 2018: 5273582. doi:10.1155/2018/5273582.

Grant, G., and W. Tabakoff. 1975. "Erosion Prediction in Turbomachinery Resulting from Environmental Solid Particles." *Journal of Aircraft* 12 (5): 471–478. doi:10.2514/3.59826.

He, W. D., C. Wang, and Y. H. Zhang. 2015. "Study of the Influence of Labyrinth Seal Clearance on Gearbox Leakage with Gas-Fluid Two-Phase Mixture." *Applied Mechanics and Materials* 789-790: 231–235 . doi:10.4028/790.231

Kim, T. S., and K. S. Cha. 2009. "Comparative Analysis of the Influence of Labyrinth Seal Configuration on Leakage Behavior." *Journal of Mechanical Science and Technology* 23 (10): 2830. doi:10.1007/s12206-009-0733-5.

Kong, X., Y. Liu, H. Lu, Z. Tian, and J. Xin. 2020. "Performance Analysis of Inter-Stage Leakage Flows at Rotating Conditions in an Axial Compressor." *Journal of Thermal Science* 29 (6): 1558–1568. doi:10.1007/s11630-020-1378-z.

Li, Z., Z. Fang, and J. Li. 2019. "Numerical Investigation on the Leakage and Rotordynamic Characteristics for Three Types of Annular Gas Seals in Wet Gas Conditions." *Journal of Engineering for Gas Turbines and Power* 141 (3): 032504.1–032504.16. doi:10.1115/gt2018-75150.

cLu, Y. J. 2016. "Gas Engine Labyrinth Oil Gas Separation Numerical Simulation Research." Master dissertation, Guangxi University.

Misiulia, D., K. Elsayed, and A. G. Andersson. 2017. "Geometry Optimization of a Deswirler for Cyclone Separator in Terms of Pressure Drop Using CFD and Artificial Neural Network." *Separation and Purification Technology* 185: 10–23. doi:10.1016/j.seppur.2017.05.025.

Tang, H. N., S. J. Wang, and J. Zhao. 2015. "Effect of Fluid-Structure Interaction on Sealed Flow Field and Leakage Rate Based on Computational Fluid Dynamics." *Journal of Shanghai Jiaotong University (Science)* 20 (3): 326–330. doi:10.1007/s12204-015-1631-x.

Wen, C., X. Cao, Y. Yang, and J. Zhang. 2012. "Evaluation of Natural Gas Dehydration in Supersonic Swirling Separators Applying the Discrete Particle Method." *Advanced Powder Technology* 23 (2): 228–233. doi:10.1016/j.apt.2011.02.012.

Wen, C., Y. Yang, J. H. Walther, K. M. Pang, and Y. Feng. 2016. "Effect of Delta Wing on the Particle Flow in a Novel Gas Supersonic Separator." *Powder Technology* 304: 261–267. doi:10.1016/j.powtec.2016.07.061.

Wu, T., and L. S. Andrés. 2019. "Leakage and Dynamic Force Coefficients for Two Labyrinth Gas Seals: Teeth-on-Stator and Interlocking Teeth Configurations. A Computational Fluid Dynamics Approach to Their Performance." *Journal of Engineering for Gas Turbines and Power* 141 (4): 0425011–04250112. doi:10.1115/1.4041123.

Zhang, Y., K. Zhang, and Y. Yao. 2019a. "Study on Oil-Gas Separation Characteristics of Gearbox Sealing System of High-Speed Electric Multiple Unit." *Computing in Science & Engineering* 1. doi:10.1109/MCSE.2019.2893305.

Zhang, Y., K. L. Zhang, and Y. Yao. 2019b. "Effect of Seal Clearance on the Separation Performance for a Gearbox Sealing System of a High-Speed Electric Multiple Unit." *Journal of Zhejiang University-Science A* 20 (5): 358–367. doi:10.1631/jzus.A1900004.

Zhu, L., A. Li, and Z. Wang. 2017. "Analysis of Particle Trajectories in a Quick-Contact Cyclone Reactor Using a Discrete Phase Model." *Separation Science and Technology* 53 (6): 928–939. doi:10.1080/01496395.2017.1386683.